Light scattering from ordered and disordered stage-1 cesium graphite

N. Caswell and S. A. Solin
The Department of Physics and The James Franck Institute,
The University of Chicago, Chicago, Illinois 60637
(Received 30 October 1978)

The Raman spectra of C_8Cs are studied at temperatures spanning the Cs melting transition at 608 K. The spectral features and their temperature dependence are incompatible with the zone-folding model of the lattice vibrations. From an analysis of the scattered-phonon frequency dependence of the Stokes–anti-Stokes ratio and the temperature dependence of the Stokes intensity it is shown that for $\omega < 600$ cm^{-1} the spectral continuum characteristic of C_8Cs arises from single phonon excitations and is not electronic in origin.

Graphite-intercalation compounds have been the subject of considerable recent research activity for both practical and fundamental reasons.[1] Much of this effort has been directed towards an understanding of the relationship between the lattice vibrations of pristine graphite and the excitations of intercalated compounds as inferred from Raman spectra. The spectra of stage-1 alkali-metal-donor intercalation compounds are qualitatively distinct from all others measured to date and have been the subject of conflicting explanations.[2,3] The distinctions are best exemplified by the compound C_8Cs.

The temperature dependence of the structure of C_8Cs samples encapsulated with an excess of cesium metal has been extensively studied using x-ray diffraction techniques.[4] At room temperature the three-dimensional (3-D) ordered structure with $\alpha\beta\gamma$ c-axis stacking[5] is confirmed and at 608 K the Cs layers melt discontinuously into an "incommensurate" liquid phase.[4] The same "excess" samples were used for x-ray studies and the light-scattering studies reported here.

The room-temperature Raman spectrum of C_8Cs is shown in Fig. 1 and consists of a continuum background on which are superposed a broad feature at $\sim$1500 cm^{-1} and sharper features at $\sim$580 cm^{-1}. It is generally agreed[2,3] that the former results from a Fano interaction[6] between a discrete state and the continuum. As can be seen from the inset of Fig. 1 the features at $\sim$580 cm^{-1} constitute a triplet of modes at 574, 594, and 620 cm^{-1} of which only those at 574 and 594 cm^{-1} have been previously observed.[3] The 620-cm^{-1} feature has been observed in many C_8Cs samples and is not spurious, i.e., a ghost, parasitic, or laser fluorescence. Also a corresponding triplet feature has been detected in C_8Rb.[7]

Dresselhaus and Dresselhaus[3] (DD) have attributed the low-energy ($\omega \leq 1000$ cm^{-1}) continuum to multiphonon excitations and the high-energy continuum to single phonon excitations whereas Nemanich, Solin, and Guerard[2] (NSG) ascribed the entire continuum to electronic excitations. In addition DD ascribed the 574-594 cm^{-1} doublet to the enlarged in-plane primitive cell of C_8Cs which results in a mapping or "zone folding" of modes with $k \neq 0$ onto the reduced Brillouin-zone center and thus to additional Raman activity. The zone-folding approach has also been applied to the electronic band structure of graphite intercalates.[8] Thus it is important to establish the circumstances under which such an approach is valid. In contrast to the zone-folding model NSG ascribed the 580-cm^{-1} features to disorder-induced first-order Raman active out-of-plane modes.

The 580-cm^{-1} features have been attributed by DD solely to in-plane zone folding in which case the three equivalent M_{1g} modes map onto $A_{1g} + E_g$ modes at the Γ point of the D_{6h} reduced zone. Thus,

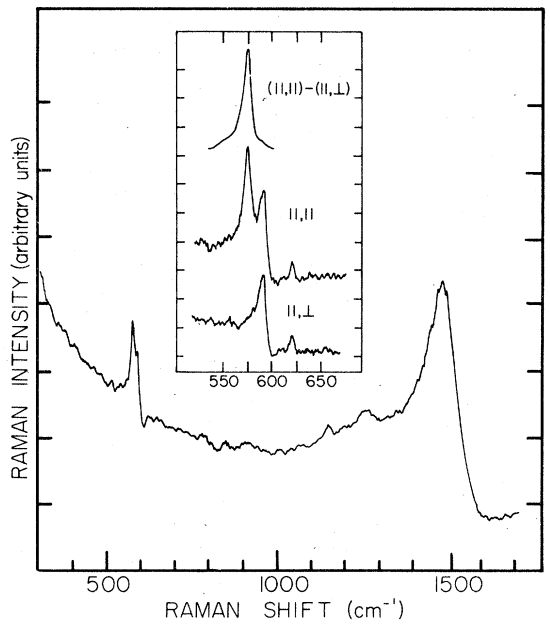

FIG. 1. Room-temperature Raman spectrum of C_8Cs.

for the backscattering Raman configuration of Fig. 1, one expects to observe one polarized and one depolarized line in the low-frequency Raman spectrum of C_8Cs. In contrast, the triplet of the insert of Fig. 1 and of C_8Rb contains two depolarized members one of which (at 594 cm^{-1}) exhibits the characteristic Fano shape.[6] The polarized member appears to be Lorentzian as can be seen from the normalized polarization difference spectrum (upper trace of insert of Fig. 1).

The essential ingredient of the zone-folding scheme is that the Raman spectrum of C_8M is a direct consequence of the ordered arrangement of intercalate atoms. Since the frequency-dependent Raman matrix elements are sensitive to an order-disorder transition one would expect significant differences in the spectra of ordered and disordered C_8Cs. Even if short-range correlations are preserved in the "incommensurate" disordered structure its Raman spectral features should be markedly broadened *vis à vis* corresponding features in the ordered phase.

In Fig. 2 we show representative Raman spectra of C_8Cs which exhibit the temperature dependence of the mode at 594 cm^{-1} for temperatures spanning the melting temperature. Also shown in the insert is the temperature dependence of the renormalized energy

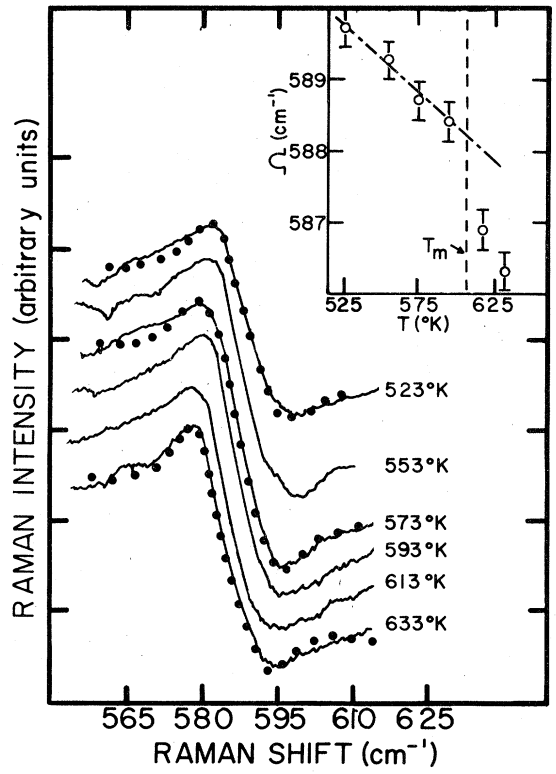

FIG. 2. Temperature dependence of the 580 cm^{-1} Fano line. (•) least-squares fit; (○) renormalized energy; (——) least-squares fit; $T_m = 608$ K is the melting temperature.

Ω deduced from a least-squares fit (solid circles) to the Raman data while the remaining Fano parameters Γ and q are temperature independent over the range of measurement and had values 0.6 ± 0.1 cm^{-1} and -1 ± 0.1. In the absence of a phase transition we expect for the temperature range given in Fig. 2 a linear dependence of Ω on T.[9] Such a linear dependence is indeed observed for $300 < T \leq 600$ K. However at $T \cong 600$ K there is a discontinuous softening of the renormalized energy. This subtle discontinuity is the only presently identifiable low-energy ($\omega \leq 600$ cm^{-1}) spectroscopic signature of the melting transition. Similar temperature insensitive behavior is exhibited by the Lorentzian line. Taken together, the spectra of Figs. 1 and 2 are incompatible with a zone-folding explanation of the vibrational excitations of C_8Cs. On the other hand if these spectra were a consequence of disorder-induced first-order scattering, they would be virtually insensitive to the melting transition as is observed. Such disorder-induced scattering could result from cesium layer defects as well as experimentally observed c-axis stacking disorder.[5]

To account for the number of bands in the disorder-induced spectra and their energies it is necessary to know the density of vibrational states and thus the phonon dispersion curves for graphite. Both have been calculated using an axially symmetric Born–von Kármán (BK) model[10,11] which is most appropriate for the in-plane modes but can be seriously in error for out-of-plane modes. For instance, the model predicts the out-of-plane zone-center A_{2u} mode at 1400 cm^{-1} while that mode is observed at 848 cm^{-1} in the ir spectrum.[12] Accordingly the M-point out-of-plane BK modes at $\approx$766 cm^{-1} most certainly have considerably smaller energies in the range of 580 cm^{-1} while the in-plane M_{1g} mode at 780 cm^{-1} should be reasonably accurate and cannot account for the 580-cm^{-1} features as required by zone folding.[13]

The above mentioned M-point out-of-plane modes of graphite generate a triplet of Raman active modes in perfectly ordered C_8Rb (space group D_{2h}^{24}) with symmetries A_g, B_{1g}, and $A_g + B_{1g}$ in order of increasing energy.[13] Such modes when disorder induced will retain their dominant symmetry characteristics and account for the polarization and ordering of the C_8Rb triplet. Similarly, the same M point modes of graphite generate at least $A_1 + 2E_2$ Raman active modes in perfectly ordered C_8Cs (space group D_6^5 or D_6^4),[7] which accounts for the disorder-induced triplet and its polarization properties in that material. Note that though the triplet polarization properties can be explained by assuming a perfectly ordered C_8M structure, the temperature dependence cannot, and indicates disorder-induced phenomena. As additional evidence for disorder-induced scattering, we also note that the features at $\approx$1150 and 1260 cm^{-1} in the spectrum of C_8Cs (Fig. 1) correspond to peaks in the

density of states of graphite.[11]

We now address the origin of the continuum background. For the backscattering configuration employed here the scattered intensity is[14]

$$I_i = \frac{R_i I_L}{\alpha_i + \alpha_L}(1 - e^{-(\alpha_i + \alpha_L)l}) \quad . \tag{1}$$

Here i = S,AS for Stokes or anti-Stokes scattering, R is the Raman efficiency, α_i (α_L) is the absorption coefficient at the scattered photon (laser photon) frequency, l is the sample thickness, and I_L is the incident intensity.

The incident photon frequency ω_L is in the Drude absorption region for C_8Cs the reflectivity of which is well accounted for with a two-carrier model.[15] Thus for backscattering

$$\alpha_M(\omega) = \frac{1}{\omega_M^2 c}\left(\frac{\omega_1(\perp)^2}{\tau_1} + \frac{\omega_2(\perp)^2}{\tau_2}\right) \equiv \frac{\bar{\omega}^2}{\omega_M^2 \tau c}, \quad M = i, L \quad , \tag{2}$$

where $\omega_1(\perp)$, τ_1, and $\omega_2(\perp)$, τ_2, are the appropriate plasma frequencies and scattering times for the two types of carrier and have been reported by Fischer.[15] Now

$$\frac{R_S}{R_{AS}} = \left(\frac{\omega_L - \omega}{\omega_L + \omega}\right)^n \left(\frac{2\omega_L - \omega}{2\omega_L + \omega}\right)^{2\delta_{1n}} e^{hc\omega/k_B T} \quad , \tag{3}$$

where energies are expressed in wave numbers, ω is the observed Raman shift and n = 4 or 1 for phonon or electron scattering, respectively,[16] and the term involving the Kronecker δ accounts for the q dependence of the electronic Raman efficiency. By substituting Eq. (2) into Eq. (1) and calculating the Stokes–anti-Stokes ratio, we find using Eq. (3) that

$$\frac{I_S}{I_{AS}}(\omega, \omega_L, T) = \left(\frac{z_-}{z_+}\right)^{n+2}\left(\frac{1+z_+^2}{1+z_-^2}\right)\left(\frac{1+z_-}{1+z_+}\right)^{2\delta_{1n}} \times \frac{1 - e^{-Q(1/z_+^2+1)}}{1 - e^{-Q(1/z_-^2+1)}} e^{hc\omega/k_B T} \quad , \tag{4}$$

where $z_\pm = 1 \pm \omega/\omega_L$ and $Q = (\bar{\omega}^2 l/\omega_L^2 \tau c)$. From Eq. (4) and the known values of Q and ω_L we can calculate the sample temperature for various shifts ω in the continuum and for a particular value of n. This procedure is summarized in Table I for a sample whose measured temperature was 400 ± 5 K as determined from two strategically placed thermocouples attached to the Pyrex capsule. The Stokes–anti-Stokes ratios given in Table I have been corrected for instrumental effects. For $\omega > 600$ cm^{-1} the anti-Stokes signal was too weak to give reliable results. The slight variation in apparent temperature with ω is not unexpected given the uncertainties in I_S/I_{AS}.

TABLE I. Comparison of sample temperature determined from Stokes–anti-Stokes ratio assuming phonon (n = 4) or electronic (n = 1) scattering.

Ω cm^{-1}	I_S/I_{AS}	n = 1	n = 4
100	1.185	467	378
200	1.376	507	408
300	1.675	459	371
400	1.903	502	405
500	2.356	461	373
600	2.719	478	387
T average		479	387
T measured		400 ± 5	

On the basis of Table I we conclude that at least for $\omega < 600$ cm^{-1} the continuum is not due to electrons but to phonons in agreement with DD.[3] (The slight temperature difference of ~10 °C between the measured and calculated temperatures may be due to radial temperature gradients in the cylindrical oven.) However the scattering process is not multiphonon as DD suggest. To show this latter point we note that the Stokes scattering intensity for an mth-phonon overtone with Raman shift ω is proportional to

$$\left[\exp\left(\frac{hc\omega}{k_B T}\right)\right] \Big/ \left[\exp\left(\frac{hc\omega}{mk_B T}\right) - 1\right]^m \quad .$$

For say ω = 400 cm^{-1} the calculated ratio

$$I_S(\omega, \omega_L, 600\ \text{K})/I_S(\omega, \omega_L, 300\ \text{K})$$

is 1.38 for m = 1, 2.62 for m = 2, and 20.27 for m = 5 whereas the observed ratio is 1.2 ± 0.2. Clearly, for $\omega < 600$ cm^{-1} the continuum is first-order phonon scattering. However at higher energies there may be a contribution to the background from interband electronic transitions.[16] From the calculated electronic band structure of C_8K,[8] we note that at T = 0 K the onset of such transitions is ~1200 cm^{-1} and involves bands along the λ line lying near the Fermi energy. We expect the C_8Cs and C_8K band structures to be similar and accordingly an electronic scattering signal for $\omega \geq 1200$ cm^{-1} may contribute to the continuum.

Zanini *et al.*[17] have employed the zone-folding model to interpret the C_6Li stage-1 Raman spectrum which contains no low-frequency features, a relatively sharp high-energy Fano band, and a weak continuum. As an alternative explanation we note that since its primitive cell contains only one carbon layer C_6Li should contain fewer c-axis stacking faults than C_8Cs. The disorder-induced scattering which results from such stacking faults would thus be significantly reduced in agreement with experiment.

In conclusion the single phonon $\omega < 600$ cm^{-1} continuum, the 1150- and 1250-cm^{-1} spectral features, and the energies, temperature dependence, number of components, and polarization properties of the 580-cm^{-1} triplet are well accounted for by disorder-induced scattering and are incompatible with the zone-folding model.

Thanks are due to Roy Clarke, R. J. Nemanich, and M. H. Cohen for useful discussions and to A. W. Moore for providing the pyrolytic graphite used in this study. Research was supported by the U.S. DOE. It has also benefitted from the support of the University of Chicago Materials Research Laboratory by the NSF.

[1]J. E. Fischer and T. E. Thompson, Phys. Today 31, No. 7, 36 (1978).
[2]R. J. Nemanich, S. A. Solin, and D. Guerard, Phys. Rev. B 16, 2965 (1977).
[3]M. S. Dresselhaus and G. Dresselhaus, in *Physics and Chemistry of Materials with Layered Structures,* edited by F. Levy (Dordrecht, Holland, 1978), Vol. 5. Also Mater. Sci. Eng. 31, 141 (1977).
[4]R. Clarke, N. Caswell, and S. A. Solin, Phys. Rev. Lett. 42, 61 (1979).
[5]D. Guerard, P. Lagrange, M. El Makrini, and A. Herold, Carbon (to be published).
[6]U. Fano, Phys. Rev. 124, 1866 (1961).
[7]N. Caswell and S. A. Solin (unpublished). At room temperature C_8K cannot tolerate sufficient incident power to provide a signal-to-noise ratio compatible with observation of the 620-cm^{-1} feature.
[8]T. Inushita, K. Nakao, and H. Kamimura, J. Phys. Soc. Jpn. 43, 1237 (1977).
[9]S. S. Mitra, in *Optical Properties of Solids* (Plenum, New York, 1969), Chap. 14.
[10]R. Nicklow, N. Wakabayashi, and H. G. Smith, Phys. Rev. B 5, 4951 (1972).
[11]R. J. Nemanich and S. A. Solin (unpublished).
[12]R. J. Nemanich, G. Lucovsky, and S. A. Solin, Solid State Commun. 23, 117 (1977).
[13]M. Maeda, Y. Kurmamoto, and C. Horie (unpublished).
[14]R. Loudon, J. Phys. 26, 677 (1965).
[15]D. Guerard, G. M. T. Foley, M. Zanini, and J. E. Fischer, Nuovo Cimento B 38, 410 (1977).
[16]*Light Scattering in Solids,* edited by M. Cardona (Springer, New York, 1975), Vol. 8., and references therein.
[17]M. Zanini, Lih-Ying Ching, and J. E. Fischer, Phys. Rev. (to be published).